A Semi-Automatic Method To Construct Atrial Fibre Structures : a Tool for Atrial Simulations

Simon Labarthe, Yves Coudière, Jacques Henry, Hubert Cochet

A Semi-Automatic Method To Construct Atrial Fibre Structures : a Tool for Atrial Simulations.

Simon Labarthe[1,2,4], Yves Coudiere[1,2,4], Jacques Henry[1,2,4], Hubert Cochet[3,4]

[1] IMB - Université Bordeaux Segalen - Université Bordeaux 1, Bordeaux, France
[2] INRIA, Bordeaux, France
[3] Department of cardiovascular imaging - CHU, Bordeaux, France
[4] Liryc Institute - CHU / Université de Bordeaux / INSERM U1045, Bordeaux, France

Abstract

Fibre structure and anisotropy is a determinant issue to provide accurate simulations of the electrical activity of atrial tissue. Though, atrial fibre architecture remains unreachable to standard imagery techniques on patients. A method to construct models of the fibre architecture on patient-specific geometries is then a key for numerical simulations of atrial tissues. Such a method is proposed. Pathological and non pathological patient specific surface models of the left atria (LA) are defined. Hence, a pathological scenario is explored : a mechanism of micro-reentry in the left superior pulmonary vein (LSPV) and its interaction with the sinus rhythm (SR).

1. Introduction

The propagation of the action potential in the heart tissue is very anisotropic. In the different mathematical models of the cardiac electrical activity, this characteristic is modelled by an anisotropic diffusion tensor field based on the underlying fibre structure of the tissue. The introduction of this anisotropy is essential to simulate accurately the activation maps and the action potential duration repartition which are key information especially for arrhythmogenic dynamics modelling[1].

However, imaging the fibre orientation is still challenging. If an accurate fibre structure on the atria can be imaged on ex-vivo hearts[1], fibres imaging tools such as DTMRI remain inefficient on in-vivo atria, owing to the weak thickness of atrial tissues. Then, constructing an a priori fibre structure from histological description [2] on a patient specific geometry is an acceptable trade-off toward patient specific simulations. We present here a new semi-automatic method that gives such an anisotropy characterisation in a semi-automatic way. A left atrium (LA) model is constructed, and a pathological fibre orientation scenario in the left superior pulmonary vein (LSPV) is tested.

2. Method

Histological descriptions [2] of the fibre structure of the LA present two main features : (1) The LA can be divided in basic **cylinder-like structures** with **circumferential** fibre orientation. (2) The variation of the fibre direction from a cylinder-like element to another is **continuous**.

Our method aims to mimic those main physiological characteristics using three steps. A surface mesh is extracted from a MR image of the LA. It is manually decomposed in cylinder-like elements which local circumferential structure is semi-automatically constructed. An in-painting algorithm extends continuously the fibre direction on the whole atrium, taking the local orientation in the basic elements as a constraint.

2.1. Imaging the LA

LA geometry was acquired in-vivo using ECG-gated contrast-enhanced multi-detector computed tomography (MDCT) in a patient with history of paroxysmal atrial fibrillation. Imaging was performed using a 64-slice CT scanner (SOMATOM Definition, Siemens Medical Solutions, Forchheim, Germany) during the intravenous injection of a 120 mL bolus of iodinated contrast agent at the rate of 4 mL/s. ECG-gating was set for acquisition window to occur at end-systole, when LA motion is minimal. Acquisition parameters were: slice thickness 0.5 mm, tube Voltage 120 kV, maximum tube current 850 mAs, and gantry rotation time 330 ms. An imaging volume comprising the whole LA was reconstructed with a voxel size of $0.5 \times 0.4 \times 0.4$ mm. Trans-axial images were imported in DICOM format in a local database of the software OsiriX 3.6.1 (OsiriX foundation, Geneva, Switzerland). The endocardial surface was segmented automatically using region growth segmentation. Volume rendering reconstructions were used to remove non atrial structures from the segmentation. Pulmonary veins (PV) were cut several cen-

timetres from their ostia. The resulting segmentation was used to compute a 3D mesh in vtk format using the software CardioviZ3D (INRIA Asclepios, Sophia Antipolis, France). The mesh was smoothed with weighted laplacian smoothing and optimized with freeYams [3] to get a mesh suitable for calculation.

2.2. Circumferential fibres

We call Ω_h the mesh representing the descretisation of Ω the endocardial surface of the imaged LA.

We identify manually using MeshLab (3D-CoForm Project, Italy) the following cylinder-like elements in Ω_h: dome, vestibule, insertions of the dome in the vestibule, PVs, auricle fingers and auricle. Some of this basic structures are clearly tubular, such as the PVs. Others can be identified as a portion of cylinder, such as the atrial dome.

After this identification, we have $\Omega = \Omega_c \cup \Omega_i$ where Ω_c is the set of all the circumferentially distributed cylinder-like zones of the LA, and Ω_i is the area to be completed by the in-painting method. Let η be the outward unit normal vector field and u be a unit vector field modelling the fibre orientation on Ω. We want $u(X)$ to be tangent to the surface for all $X \in \Omega$. To impose this characteristic, we compute the vectorial product $u = u^* \wedge \eta$ where u^* is an adjoint vector field that is to construct.

To construct circumferential fibres on a given cylinder-like basic element ω of Ω_c, we need to obtain the vector field $u^*_{|\omega}$ which should be closed to the "axis" of ω.

In that goal, an usual method in vascular imaging [4] is performed : we search for the rotation axis that minimizes the inertia momentum of the structure by a spectral analysis of the inertia matrix.

Let ω_h be the mesh resulting from the discretization of ω and Δ a line through the origin O. ω_h is considered as a non-deformable homogeneous geometry with a uniform surface mass of 1. The inertia momentum $I_\Delta(\omega_h)$ of ω_h respectively to a rotation around the axis Δ supported by a unit vector e_Δ can be written :

$$I_\Delta(\omega_h) = \sum_{p_i \in \omega_h} R_{p_i}^2$$

where R_{p_i} is the distance between the point $p_i \in \omega_h$ and Δ.

For all $p_i \in \omega_h$, $R_{p_i}^2$ can be calculated with the formula

$$R_i^2 = (e_\Delta \wedge P_i).(e_\Delta \wedge P_i)$$

where $P_i = (x_i, y_i, z_i)$ is the coordinates vector of the point p_i. $I_\Delta(\omega_h)$ can be rewritten as follows

$$I_\Delta(\omega_h) = e_\Delta.I(\omega_h)e_\Delta$$

with $\quad I(\omega_h) = \begin{pmatrix} \sum_i y_i^2 + z_i^2 & \sum_i x_i y_i & \sum_i x_i z_i \\ \sum_i x_i y_i & \sum_i x_i^2 + z^2 & \sum_i y_i z_i \\ \sum_i x_i z_i & \sum_i y_i z_i & \sum_i x_i^2 + y_i^2 \end{pmatrix}$ the inertia matrix of ω_h.

$I(\omega_h)$ is a real symmetric matrix. Let $\alpha(\omega_h)$ be the smallest eigenvalue of $I(\omega_h)$ and $e_\alpha(\omega_h)$ a corresponding unit eigenvector. Then, $e_{\alpha(\omega_h)}$ is the direction of the axis $\alpha(\omega_h)$ that minimizes the inertia momentum of the rotation of Ω_h. For a cylinder $\mathcal{C}$, $e_{\alpha(\mathcal{C})}$ corresponds to the axis of $\mathcal{C}$.

We set $u^*_{|\omega_h} = e_{\alpha(\omega_h)}$ and we construct $u_{|\omega_h} = u^*_{|\omega_h} \wedge \eta_{|\omega_h}$. A result of this step can be seen in figure 1.

If the the shape of the initial component is too far from a cylinder, this method may not give acceptable results : a manual correction must be performed using linear combination of the three eigenvectors.
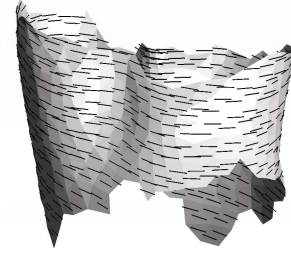

Figure 1. Result of the fibre construction on the base of the left superior pulmonary vein.

2.3. Completion using an in-painting method

The second step of the method consists in completing continuously the fibre structure u outside the basic cylindrical elements.

Inpainting PDE methods usually recursively perform a smoothing procedure on an initial distribution on the whole domain Ω until a convergence criteria is reached - see [5] for a short review of in-painting methods adapted to fibre reconstruction. We use here an adaptation of the laplacian smoothing algorithm which is easier to implement and compute than more sophisticated algorithms such as Sobolev or total variation smoothing. In counterpart, we don't have here the optimal regularity guaranteed by those algorithms.

We perform the inpainting algorithm on the adjoint vector field u^* which may be more regular than the fibre vector field. Let $\Omega_{i,h}$ the discretization of Ω_i and $U^*_{|\Omega_i}$ the discrete version of the adjoint vector field $u^*_{|\Omega_i}$ that we want to construct. This vector has dimension N_T, where N_T is the number of triangles in $\Omega_{i,h}$.

We define U^{*^0} the matrix of dimension $N_T \times 3$ such that $U^{*^0}_j = (1, 0, 0)$ for all $j \in [1, N_T]$. We construct recur-

sively a family of vector fields with the following process :

$$\forall n > 0, \forall j \in [1, N_T], U_j^{*^n} = \frac{\sum_{k=1}^{3} U_{\varphi(j,k)}^{*^{n-1}}}{|| \sum_{k=1}^{3} U_{\varphi(j,k)}^{*^{n-1}} || + \epsilon_0}$$

where ϵ_0 is a small regularisation parameter that prevents an indetermination when $|| \sum_{k=1}^{3} U_{\varphi(j,k)}^{*^{n-1}} ||$ vanishes. $\varphi(j, k)$ is the index in $\Omega_{i,h}$ of the kth of the three triangles sharing an edge with the jth triangle of $\Omega_{i,h}$. If the jth triangle is on the boundary of $\Omega_{i,h}$, some of this neighbour triangles are not included in $\Omega_{i,h}$ but in $\Omega_{c,h}$. Then, $\varphi(i, j)$ is the index in $\Omega_{c,h}$ of such a triangle, and $U_{\varphi(i,j)}^{*^{n-1}}$ is the value of the adjoint vector field already defined in the previous step of the method. This algorithm is stopped when

$$||(||U_j^{*^n} - U_j^{*^{n-1}}||_{l^2})_{j \in [1,N_T]}||_{l^\infty} < \epsilon$$

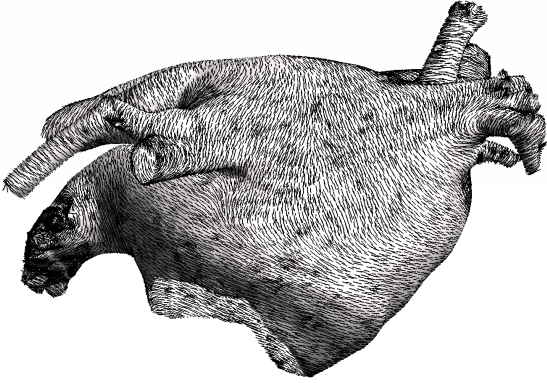A result of the fibre organisation given by this method in the whole LA can be seen in figure 2.

Figure 2. Result of the fibre direction construction process on the LA. Postero-inferior view.

3. A tool for simulations

This model of LA is used to perform simulation of a pathological situation. We study the interaction between several beats of sinus rhythm and a micro-reentry in LSPV triggered by a fibre direction heterogeneity.

3.1. Simulation method

We solve the monodomain equation with a P1 finite element method using an implicit Euler scheme. We set the surface capacity of the cells to 1 μF.cm^{-2} and the cell surface to volume ratio to 250 cm^{-1} to ensure propagation speed comparable to [6].

Fibres orientation : we use the atrial fibre orientation model previously defined with a specific fibre structure in the LSPV inspired of a scenario presented in [7] : the fibre orientation is circumferential in the distal part of the vein, whereas it's tangential in the ostial part, with an abrupt change of fibre direction between those structures, excepted in a transition zone - figure 3. This complex structure is constructed by adapting our method : the spectral analysis is used in the ostial and distal part, while inpainting is computed for the transition zone.
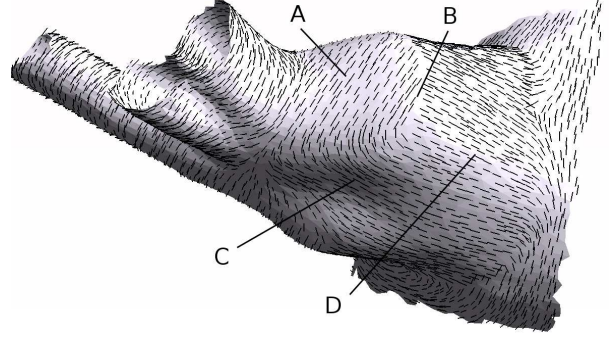

Figure 3. Pathological fibre structure in the LSPV. A - circumferential orientation in the distal zone. B - steep transition zone. C - smooth transition zone. D - tangential orientation in the ostial zone.

Conductivity : We set the longitudinal conductivity to 1.5 mS.cm^{-1} in the whole LA and the transverse conductivity to 0.24 mS.cm^{-1}, except for the pectinate muscles of the appendage that are set to 0.6 mS.cm^{-2} to model a more isotropic area triggered by the less regular fibre structure. The LSPV is given a longitudinal and transverse conductivity of respectively 1.6 mS.cm^{-1} and 0.02mS.cm^{-1} to ensure a conduction block at the fibre heterogeneity.

Electrophysiology : We use the the Courtemanche-Ramirez-Nattel (CRN) model to simulate the atrial electrophysiology. We apply multiplicative factors on g_{Na}, g_{Kl}, g_{to} and $g_{Ca,l}$, with a value of respectively 1.1, 1.9, 0.74 and 0.85 in the LA and 0.42, 2.7, 0.6, 0.85 in the LSPV. Those factors shorten the action potential (AP) and increase the spreading velocity in the LA whereas they give a triangular shape to the AP and decrease the velocity in the LSPV.

Initial stimulations : we simulate the main inter-atrial connexions. We apply a stimulation current in, successively, the Bachmann's bundle insertion (BBI), in the coronary sinus (CS) and in the fossa ovalis (FO) that model the sinus wave spreading in the LA. Activation of CS and FO is delayed of respectively 21ms [6] and 5ms, comparatively to the BBI which is stimulated with a period of 400ms. Two ectopic beats are applied in the distal part of the LSPV 113ms before and 64 ms after the BBI.
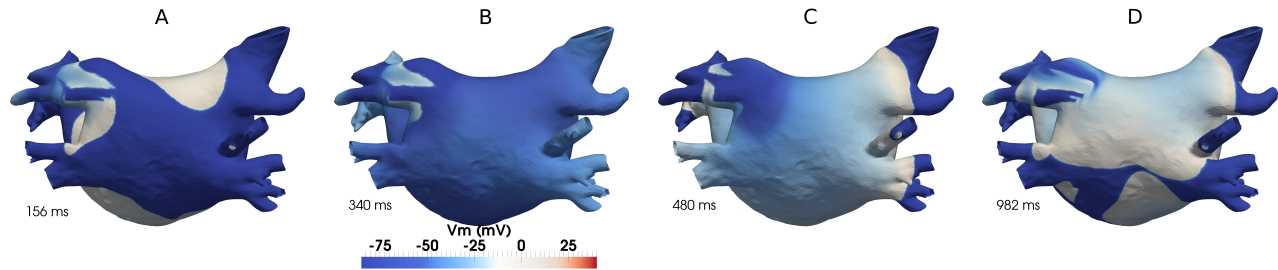
Figure 4. Potential maps in a posterior view of LA. Dark blue : resting potential. Light-beige : depolarisation front. A, 156 ms: the first ectopic wave in the LSPV invades the transition zone to meet the sinus wave coming from BB (top) and CS (bottom). B, 340 ms : the second ectopic wave is coming into the repolarising ostial part through the transition zone. C, 460 ms : the first loop of the micro-reentry anchored in the discontinuity zone of the LSPV gets into the repolarising tissue of the last ectopic wave. The loop period of the micro-reentry is about 163 ms. D, 982 ms : the micro-reentry wave collides with the sinus wave from BB (top), surrounds the ostium of the left inferior pulmonary vein and meets the sinus wave from CS.

3.2. Simulation results

The front of the sinus wave is distorted by the anisotropy of the conductivity field so that preferential paths are taken: from the BB and CS to the vestibule and the roof of the LA, in a very comparable way than [1, 8]. The ectopic wave front is extremely slowed by the electrophysiological characteristic set in the LSPV, so that the sinus wave and the ectopic wave meet together in the ostial part of the LSPV. A micro-reentry is triggered in the LSPV by the second ectopic beat (figure 4) : the ectopic wave is stopped distally by the fibre discontinuity zone, invades the proximal part through the transition zone and goes back in the distal part when the tissue has recovered. The micro-reentry perturbs the sinus wave during the next beats.

4. Discussion and conclusion

We presented a new method to characterise the anisotropy on patient-specific LA surface models. This method is able to reproduce in an interactive and semi-automatic way the main structures of fibre direction in LA as described in [2]. However, this fibre structure is not patient dependant : it's *a priori* defined from a description of the mean fibre direction in the LA. This method is still time-demanding, mainly because of the multiple software that were used : a more integrated tool could be designed. Nevertheless, it may be a more flexible tool than the previous method proposed in [8] : in particular, it can create complex local fibre structures in a straightforward manner. One scenario was implemented : it triggered micro-reentries in the LSPV that perturbed the sinus rhythm.

Acknowledgements

References

[1] Zhao J, Butters TD, Zhang H, Pullan AJ, LeGrice IJ, Sands GB, Smaill BH. An image-based model of atrial muscular architecture / clinical perspective. Circulation Arrhythmia and Electrophysiology 2012;5(2):361–370.

[2] Ho S, Sanchez-Quintana D, Cabrera J, Anderson R. Anatomy of the left atrium: implications for radiofrequency ablation of atrial fibrillation. Journal of Cardiovascular Electrophysiology 1999;10(11):1525 – 1533. ISSN 1045-3873.

[3] Frey P. About surface remeshing. In Proc. 9th Int. meshing Roundtable, NewOrleans. 2000; .

[4] Hernandez-Hoyos M. Segmentation anisotrope 3D pour la quantification en imagerie vasculaire par résonance magnétique. Ph.D. thesis, INSA de Lyon, 2002.

[5] Rousseau O. Geometrical Modeling of the Heart. Ph.D. thesis, University of Ottawa, Ottawa-Carleton Institute for Mathematics and Statistics, 2009.

[6] Harrild DM, Henriquez CS. A computer model of normal conduction in the human atria. Circ Res 2000;87(7):e25–36.

[7] Zemlin CW, Mitrea BG, Pertsov AM. Spontaneous onset of atrial fibrillation. Physica D Nonlinear Phenomena 2009; 238(11-12):969 – 975. ISSN 0167-2789.

[8] Krueger MW, Schmidt V, Tobón C, Weber FM, Lorenz C, Keller DUJ, Barschdorf H, Burdumy M, Neher P, Plank G, Rhode KS, Seemann G, Sanchez-Quintana D, Saiz J, Razavi R, Dössel O. Modeling atrial fiber orientation in patient-specific geometries: A semi-automatic rule-based approach. In FIMH'11. 2011; 223–232.

Address for correspondence:

Simon Labarthe
Inria,200 avenue de la Vieille Tour, 33405 Talence Cedex, France
simon.labarthe@u-bordeaux2.fr